A simple accurate method to predict time of ponding under variable intensity rainfall

S. Assouline,[1,2] J. S. Selker,[1,3] and J.-Y. Parlange[1,4]

Received 1 May 2006; revised 17 September 2006; accepted 12 October 2006; published 16 March 2007.

[1] The prediction of the time to ponding following commencement of rainfall is fundamental to hydrologic prediction of flood, erosion, and infiltration. Most of the studies to date have focused on prediction of ponding resulting from simple rainfall patterns. This approach was suitable to rainfall reported as average values over intervals of up to a day but does not take advantage of knowledge of the complex patterns of actual rainfall now commonly recorded electronically. A straightforward approach to include the instantaneous rainfall record in the prediction of ponding time and excess rainfall using only the infiltration capacity curve is presented. This method is tested against a numerical solution of the Richards equation on the basis of an actual rainfall record. The predicted time to ponding showed mean error $\leq$7% for a broad range of soils, with and without surface sealing. In contrast, the standard predictions had average errors of 87%, and worst-case errors exceeding a factor of 10. In addition to errors intrinsic in the modeling framework itself, errors that arise from averaging actual rainfall records over reporting intervals were evaluated. Averaging actual rainfall records observed in Israel over periods of as little as 5 min significantly reduced predicted runoff (75% for the sealed sandy loam and 46% for the silty clay loam), while hourly averaging gave complete lack of prediction of ponding in some of the cases.

Citation: Assouline, S., J. S. Selker, and J.-Y. Parlange (2007), A simple accurate method to predict time of ponding under variable intensity rainfall, *Water Resour. Res.*, *43*, W03426, doi:10.1029/2006WR005138.

1. Introduction

[2] When water is applied to the soil surface, it infiltrates until the application rate exceeds the soil-limited infiltration rate, when ponding occurs at the soil surface, and runoff and erosion can be initiated. The ability to estimate accurately when initial ponding occurs and how much runoff is produced is important in civil and agricultural engineering, and is essential for the proper design of irrigation systems, rain harvesting reservoirs, and hydraulic structures at the level of the watershed.

[3] Infiltration is a complex phenomenon controlled by a series of factors. In principle, local infiltration is ruled by the actual hydraulic properties of the soil profile, the rainfall intensity, and the water content distribution with depth. These basic factors hold when one extends the analysis to infiltration in locally nonuniform soil profiles or spatially varying systems at the scale of the field or the watershed. A large body of research has shown that spatial variability of soil properties affect infiltration at such scale [*Russo and Bresler*, 1982; *Sivapalan and Wood*, 1986; *Saghafian et al.*, 1995]. The effect of local heterogeneity within the soil profile on infiltration was also demonstrated for layered or nonuniform soils, mainly relying on the *Green and Ampt* [1911] approach [*Childs and Bybordi*, 1969; *Beven*, 1984; *Selker et al.*, 1999; *Chu and Marino*, 2005]. A special case of soil nonuniformity is when a seal layer develops at the soil surface due to the raindrop impacts [*Assouline*, 2004]. Infiltration through such nonuniform soil profiles was also modeled [*Hillel and Gardner*, 1970; *Ahuja*, 1983; *Parlange et al.*, 1984; *Baumhardt et al.*, 1990; *Assouline and Mualem*, 1997]. Recently, *Chu and Marino* [2005] have presented a modified Green and Ampt model that deals with infiltration into layered soils under unsteady rainfall. In their model the time to ponding can be identified only if all the infiltration process is solved step by step and the cumulative infiltration computed according to the rainfall time discretization. The combined effect of soil spatial variability and profile heterogeneity on infiltration was studied by *Assouline and Mualem* [2002]. The main result is that accounting for soil surface sealing has a greater effect on infiltration than accounting for soil spatial variability.

[4] Spatial and temporal variability in rainfall or water application rates also affect infiltration. A constant rate supply of water may well represent sprinkler irrigation, however temporal variability is ubiquitous in rainfall with clear influence on runoff and erosion estimates [e.g., *Agnese and Bagarello*, 1997; *Wainwright and Parsons*, 2002; *Frauenfeld and Truman*, 2004; *Strickland et al.*, 2005; *Govindaraju et al.*, 2006]. *Agnese and Bagarello* [1997] found that the temporal resolution required for the accurate

[1]Institute of Environmental Science and Technology, School of Architecture, Civil and Environmental Engineering, Ecole Polytechnique Fédérale de Lausanne, Lausanne, Switzerland.
[2]On leave from Institute of Soil, Water and Environmental Sciences, Agricultural Research Organization, Volcani Center, Bet Dagan, Israel.
[3]On leave from Department of Biological and Ecological Engineering, Oregon State University, Corvallis, Oregon, USA.
[4]On leave from Department of Biological and Environmental Engineering, Cornell University, Ithaca, New York, USA.

0043-1397/07/2006WR005138

prediction of infiltration was strongly dependent on the soil type, and that its effect was practically negligible for soils with either high or low permeability. *Wainwright and Parsons* [2002] concluded that overland flow models that account for run-on infiltration underpredict runoff when the mean rainfall intensity is used instead of time-varying rainfall intensity. Efforts are now invested in modeling infiltration under variable rainfall intensity. *Govindaraju et al.* [2006] suggested a semianalytical model to compute the space-averaged infiltration at hillslope scale when spatial variability in both soil property and rainfall intensity are accounted for. The soil spatial heterogeneity is characterized by a lognormal distribution of the saturated hydraulic conductivity, while the rainfall spatial heterogeneity is simulated by a uniform distribution between two extreme rainfall intensities. At each location, the soil saturated hydraulic conductivity and the rainfall intensity was assumed to remain constant during the rainfall event. The results of this model are in agreement with those of *Assouline and Mualem* [2002] for the unsealed (mulched) soil surface case.

[5] On the basis of this literature review, we focus, in this paper, on the processes of local infiltration and ponding occurrence for variable water application rates at the surface of both a homogeneous soil and a heterogeneous one represented by a sealed profile.

[6] During infiltration under shallow ponding (i.e., where infiltration is not strongly affected by the depth of ponding) the infiltration capacity rate, f_{cap}, decreases due to the decrease of the hydraulic head gradient resulting from the advancement of the wetting front. The infiltration capacity curve, $f_{cap}(t)$, can be thus considered a soil characteristic with dependence on the initial soil water content profile, which can be relatively easily characterized under laboratory or field conditions. When water is applied at a prescribed rate, for example under low rainfall intensity or sprinkler or drip irrigation, all of the supplied water infiltrates into the soil until ponding occurs, whence the actual rate of infiltration, f, is controlled by the soil infiltration capacity until the application rate falls below it. The temporal history of the actual infiltration $f(t)$, unlike $f_{cap}(t)$, is a function of the pattern of water application.

[7] The importance of the infiltration process in soil, hydrology, and environmental sciences had led to considerable literature dealing with experimental observations, and theoretical, analytical, numerical and empirical modeling of infiltration [e.g., *Clothier*, 2001; *Warrick*, 2002; *Smith et al.*, 2002; *Hillel*, 2004; *Brutsaert*, 2005; *Hopmans et al.*, 2006]. Analytical and empirical mathematical expressions have been proposed to provide a quantitative description of $f_{cap}(t)$ and $f(t)$ [e.g., *Green and Ampt*, 1911; *Kostiakov*, 1932; *Horton*, 1940; *Philip*, 1957a; *Smith and Parlange*, 1978; *Parlange et al.*, 1999]. From these results expressions have been derived to estimate the time when ponding occurs, t_p [e.g., *Chow et al.*, 1988; *Kutilek and Nielsen*, 1994; *Parlange et al.*, 1999; *Smith et al.*, 2002; *Brutsaert*, 2005]. Although being theoretically valid for unsteady rainfall, most of its practical applications (1) have assumed that water is supplied at a constant rate or consider the time-averaged rate of supply until ponding, (2) have neglected the effect of raindrop impact on the soil surface when a bare soil is exposed to high-energy rainfall, and (3) do not account for the antecedent water distribution. These restrictions do not allow accurate representation for many situations.

[8] Once t_p is evaluated, the second important need is prediction of $f(t)$ after ponding, essential for prediction of processes governed by runoff (e.g., floods and erosion). Methods widely used are the time compression approximation (TCA) [*Brutsaert*, 2005], or the infiltrability-depth approximation (IDA) [*Smith et al.*, 2002]. The TCA was introduced in the 1940s [*Sherman*, 1943; *Holtan*, 1945] and has been applied widely [e.g., *Reeves and Miller*, 1975; *Sivapalan and Milly*, 1989; *Kim et al.*, 1996]. It relies on the assumption that infiltration rate after ponding is a unique function of the cumulative infiltration volume, F. For $t < t_p$, $F(t)$ is equal to the cumulative rainfall, $R(t) = \int_0^t r(t)dt$. One may define the cumulative infiltration capacity, $F_{cap}(t) = \int_0^t f_{cap}(t)dt$, and a compression reference time, t_{cr}, which is the time required to produce the same cumulative infiltration volume under shallow ponding conditions from $t = 0$. Thus $F(t_p) = R(t_p) = F_{cap}(t_{cr})$. Once t_p and t_{cr} are known, $f(t)$ for continued ponding can be evaluated as $f_{cap}(t - t_0)$, with $t_0 = (t_p - t_{cr})$. It is evident that the TCA requires an accurate estimate of t_p and t_{cr}. As was true for t_p, the available expressions for estimation of t_{cr} assume either constant or time-averaged wetting rate [*Brutsaert*, 2005] which limits the practical utility of this approach.

[9] On the basis of numerical calculations, *Smith* [1972] and *Smith and Chery* [1973] suggested an implicit computation of t_p:

$$\left(\frac{r_p}{K_s} - 1\right)^{\beta-1} \int_0^{t_p} r dt = A \tag{1}$$

where $r(t)$ is the observed rainfall rate which is required to be at most slowly varying close to t_p; r_p is the rainfall rate at t_p; A is a linear function of the initial water content assumed constant with depth in the soil profile; K_s is the saturated hydraulic conductivity; and β is a parameter found to be close to 2. *Parlange and Smith* [1976] proposed an alternative expression which requires one less parameter that can be applied for any rainfall pattern for which $r_p < K_s$:

$$\frac{\int_0^{t_p} r dt}{\ln\left[\frac{r_p}{(r_p - K_s)}\right]} = \frac{S^2}{2K_s} \tag{2}$$

where S is the soil sorptivity. *Broadbridge and White* [1987] developed an expression similar to equation (2) for t_p for the case of rainfall events characterized by a linear increase in r with t. Insight on the physics leading to these expressions can be found in the literature on infiltration [e.g., *Clothier*, 2001; *Warrick*, 2002; *Smith et al.*, 2002; *Hillel*, 2004; *Brutsaert*, 2005; *Hopmans et al.*, 2006].

[10] These expressions are implicit functions where the unknown variable is t_p, and require that soil sorptivity and hydraulic conductivity be known. This is a significant constraint for field conditions where heterogeneity, anisotropy, and/or preferential flow make these parameters difficult to obtain. One related point is the effect of surface condition on soil properties and consequently, on infiltration

and runoff. When a bare soil surface is exposed to rainfall, the energy of the raindrop impacts lead to soil surface sealing. This process can significantly reduce the infiltration rate, and consequently the time to ponding [*Assouline*, 2004]. Here the influence of surface sealing is evaluated through comparison with an unsealed soil surface (denoted herein as "mulched," since this would typically occur only if the surface was mechanically protected from raindrop impact).

[11] The above mentioned expressions were developed in a context where rainfall data were available mainly on a daily basis, for which taking the rainfall intensity to be constant was reasonable. In the past decade the use of electronically recording tipping bucket, radar rainfall estimates, and desdrometers has made high temporal resolution rainfall data widely available. It is therefore timely to have a simple method for estimating t_p that can readily be applied to complex rainfall patterns. It is further of considerable interest to study the effect of the time-averaging interval on ponding and runoff estimates to understand how the rainfall reporting interval affects t_p estimates.

[12] Infiltration, time to ponding, and runoff generation are considered as they manifest in three soils simulated to have been exposed to a natural rainfall event with highly variable intensity. The specific focus here is put on estimation of t_p considering (1) the effect of the time interval for averaging rainfall intensity data and (2) the effect of the soil surface sealing. A simple, direct method for estimating t_p for any pattern of temporal variation in rainfall intensity is presented in comparison to direct numerical simulations. The study does not intend to be comprehensive, with the important considerations of initial water content distribution, hysteresis in water retention, hydrophobicity and soil swelling being not included. However, relying on the results of *Assouline and Mualem* [2002] and *Govindaraju et al.* [2006], the method can be directly applied to space-averaged infiltration when spatial variability in soil and rainfall are accounted for.

2. Direct Method for Estimating t_p and Infiltration After Ponding

[13] We seek an explicit method to compute the time to ponding using arbitrarily time varying rainfall rate. Until ponding

$$F(t) = R(t) \qquad \text{for } t \le t_p. \tag{3}$$

[14] Thereafter, in accordance with the framework of TCA/IDA [*Smith et al.*, 2002; *Brutsaert*, 2005], it is assumed that for the period of ponding, the actual infiltration rate is a one-to-one function of cumulative infiltration. On the basis of numerical simulations, this assumption has been shown to be valid in the cases of homogeneous and layered soil profiles [*Smith*, 1990], as well as for sealed soil profiles [*Mualem and Assouline*, 1996; *Assouline and Mualem*, 2001]. Adopting this assumption we may now define the postponding infiltration rate as

$$f(F) = f_{cap}\left(F_{cap}\right) \qquad \text{for } t > t_p \tag{4}$$

[15] Therefore, at the moment ponding occurs,

$$r(R) = f(F) = f_{cap}\left(F_{cap}\right) \qquad \text{at } t = t_p \tag{5}$$

[16] The time to ponding, t_p, is thus the time when the condition $r(R) = f_{cap}(F_{cap})$ is fulfilled:

$$t_p = t\left[R\left(r = f_{cap}\right)\right] \tag{6}$$

[17] Since the function F_{cap} is obtained directly from the known f_{cap} and R is measured, equations (5) and (6) are in essence equivalent and allow direct calculation of t_p.

[18] This calculation is valid for any rainfall pattern. Many mathematical expressions are available for $f_{cap}(t)$ [e.g., *Green and Ampt*, 1911; *Kostiakov*, 1932; *Horton*, 1940; *Philip*, 1957a; *Smith and Parlange*, 1978; *Parlange et al.*, 1999], most of which can be readily adapted to represent $f_{cap}(F_{cap})$. Alternatively, simple expressions can be fitted to measured f_{cap} data. For the cases where the rainfall patterns are simple and $r(R)$ and $t(R)$ can be described mathematically, closed form expressions of t_p can be developed based on equation (6). For example, $f_{cap}(F_{cap})$ can be described by means of

$$f_{cap}\left(F_{cap}\right) = \beta\left(\frac{1 + F_{cap}}{F_{cap}}\right) \tag{7}$$

where β is a soil-dependent parameter. Using equation (6) for a constant rainfall intensity case leads to

$$t_p = \frac{\beta}{r(r-1)} \tag{8}$$

[19] Similarly, but now describing $f_{cap}(F_{cap})$ by means of

$$f_{cap}\left(F_{cap}\right) = \left(1 - e^{-\gamma F_{cap}}\right)^{-1} \tag{9}$$

where γ is a soil-dependent parameter, leads to

$$t_p = \frac{\gamma^{-1}}{r} \ln\left(\frac{r}{r-1}\right) \tag{10}$$

[20] For convenience time and rainfall rate can be rescaled following *Brutsaert* [2005]:

$$t_+ = \frac{K_s^2 t}{S^2} \;;\; r_+ = \frac{r}{K_s} \tag{11}$$

[21] The expressions in equations (8) and (10), when t, r and t_p are replaced by t_+, r_+ and t_{p+}, are therefore identical to the normalized forms of the relationships suggested for t_p when the infiltration models of *Green and Ampt* [1911] or *Parlange and Smith* [1976] are used [*Smith et al.*, 2002].

[22] The infiltration rate after ponding is given in equation (4). The difference between the actual rainfall rate and the infiltration rate is referred to as the rainfall excess representing the potential runoff rate, q:

$$q(t) = r(t) - f[t(R)] = r(t) - f_{cap}[R(t)] \tag{12}$$

[23] The only assumption made here is that after ponding the infiltration rate is a unique function of cumulative infiltration. It does not require, for example, any of the assumptions made to describe the $f_{cap}(t)$ relationships that

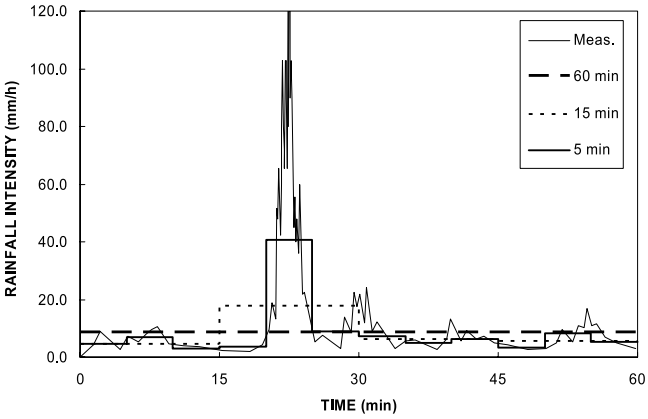

Figure 1. Measured temporal intensity of the rainfall event and the corresponding variation for three aggregation time intervals: 5, 15, and 60 min.

led to the previous expressions of t_p [*Smith et al.*, 2002; *Brutsaert*, 2005]. This method does not require specific computation of the soil properties K_s and S, though these might be fit to the $f_{cap}(t)$ function, or conversely $f_{cap}(t)$ could be computed if the soil properties are known. It is further noteworthy that this method is valid for any time-varying rainfall pattern. The infiltration after ponding predicted by equation (4) does not require the evaluation of the compression reference time, t_{cr}, avoiding additional sources of errors. Of interest in this study is the feature that the method allows for direct computation of the possible impact of the time aggregation of rainfall data on infiltration, ponding time, and runoff estimates.

3. Methodology

[24] Three soil types with widely differing hydraulic properties were selected: Sharon sandy loam (SL); Ruhama loam (L); and Atwood silty clay loam (SCL). These soils were chosen because they are well characterized for infiltration, including having hydraulic properties of the respective seal layers that develop during exposure to rainfall [*Assouline and Mualem*, 1997; *Assouline*, 2004].

[25] The data of the rainfall event chosen to represent the temporal variation of the rainfall intensity is presented in Figure 1. This event occurred on 18 December 2003 at Ramat Hacovesh, central Israel, and represent typical events during the rainy season in this region of semiarid climate. It was measured using a tipping bucket, for which each tip was calibrated to correspond to 0.1 mm of rainfall. We employ the first 60 min of the storm during which rainfall intensity varied from 2.0 to 120.0 mm/h. For the analysis of temporal averaging these data were then aggregated into 5 min, 15 min and 60 min averages.

[26] Infiltration into undisturbed soil profiles, representing the case where the soil surface is protected from the raindrop impacts by mulch, and into soil profiles over which a seal layer had formed were simulated using HYDRUS-1D [*Simunek et al.*, 2005]. The *van Genuchten* [1980] expression for the water retention curve, and *Mualem*'s [1976] model for the hydraulic conductivity function were used. In the case of the sealed soil profiles, the surface hydraulic properties used were those determined by *Assouline and Mualem* [1997] which employ the *Brooks and Corey* [1964] expression for the retention curve. The parameters for the *van Genuchten* [1980] model were determined by fitting retention data over the 0 to −200 cm capillary head range (Table 1). The seal layer thickness was taken to be 4.0 cm, and the depth of the simulation domain was 100 cm, which was sufficient to assure that the wetting processes did not come in contact with the lower boundary. The upper boundary condition switched from a Neuman condition to a Dirichlet condition after ponding. The lower boundary was assumed to be a free drainage boundary. Initial capillary head of −100 cm was applied to the whole profile. Time discretizations were as follows: initial time step, 0.5 min; minimum time step, 0.014 min; and maximum time step, 1.0 min. HYDRUS-1D was also used to generate the infiltration capacity curves, $f_{cap}(t)$, for the different soils and surface conditions. In that case the upper boundary condition was a Dirichlet condition for the whole simulation. The resulting $f_{cap}(t)$ curves for the three soils and the two soil surface conditions are depicted in Figure 2, and present a wide range of soil infiltrability. The model of *Philip* [1957b] was fitted to f_{cap} (t) to estimate the sorptivity, S.

4. Results and Discussion

4.1. Direct Method for Estimating t_p

[27] The performance of the TCA method is illustrated in Figure 3 for the three soils and the case of the sealed profiles

Table 1. Parameters of the Hydraulic Properties of the Mulched (Undisturbed) Soils and of Their Respective Seal Layers[a]

Soil	S^2, cm^2 min^{-1}	K_s, cm min^{-1}	θ_s, m^3 m^{-3}	θ_r, m^3 m^{-3}	α, cm	n
Atwood silty clay loam (SCL)						
Mulched (m)	2.55 10^{-2}	1.17 10^{-2}	0.420	0.225	0.0137	1.716
Seal (s)	1.41 10^{-3}	7.00 10^{-4}	0.397	0.236	0.0114	1.789
Ruhama loam (L)						
Mulched (m)	3.00 10^{-1}	7.50 10^{-2}	0.440	0.148	0.0093	2.392
Seal (s)	1.41 10^{-3}	6.50 10^{-4}	0.418	0.189	0.0061	2.801
Sharon sandy loam (SL)						
Mulched (m)	7.17 10^{-1}	1.67 10^{-1}	0.430	0.072	0.0179	2.299
Seal (s)	9.00 10^{-3}	2.12 10^{-3}	0.408	0.096	0.0111	2.395

[a] S is the soil sorptivity; K_s, the saturated hydraulic conductivity; θ_s and θ_r, the saturated and residual water content; and α and n, the parameters in the *van Genuchten* [1980] expression for the water retention curve.

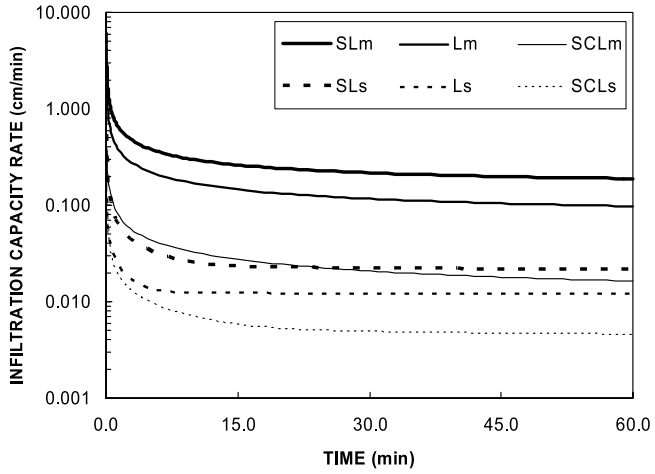

Figure 2. Infiltration capacity curves, $f_{cap}(t)$, for the three soils (SCL, SL and L) with the two soil surface conditions (m for "mulched" and s for "sealed" soil surface).

as they all produce runoff for the rainfall event. The ponding time, t_{pcal} and the compression reference time, t_{crcal} are estimated according to the expressions suggested by *Brutsaert* [2005]:

$$t_{pcal} = \frac{S^2}{2\bar{r}_p K_s} \ln\left(\frac{\bar{r}_p}{\bar{r}_p - K_s}\right) \tag{13}$$

$$t_{crcal} = \left[-a + \left(a^2 + \bar{r}_p b t_{pcal}\right)^{1/2}\right]^2 / b^2 \tag{14}$$

where S is the sorptivity; K_s is the saturated hydraulic conductivity of the seal; $\bar{r}_p$ is the mean rainfall intensity prior to ponding; and a and b, the fitting parameters of *Philip* [1957b] equation to f_{cap} (t) (with $a = S/2$). Note that equation (13) follows from equation (2) if r_p is replaced by $\bar{r}_p$. Values of variables obtained using the simulation model will be identified by subscript "*sim*" while those calculated by either traditional or the proposed method will be identified by subscript "*cal*". In Figure 3 the cumulative measured rainfall depth, $R(t)$, and the simulated cumulative infiltration, $F_{sim}(t)$ curves are becoming distinct at the simulated ponding time t_{psim}. Also depicted in Figure 3 are the cumulative $F_{cap}(t)$ and the cumulative $F_{cap}(t - t_{0cal})$ curves, with $t_{0cal} = (t_{pcal} - t_{crcal})$. According to the TCA method, (1) the estimated ponding time, t_{pcal}, is at the intersection between the $R(t)$ and $F_{cap}(t - t_{0cal})$ curves, and (2) the cumulative infiltration after ponding should be represented by $F_{cap}(t - t_{0cal})$. It can be seen that the TCA predictions conclusively failed for the SL and the L soil cases. In the first one, it overestimated t_{psim} with an error of 64%, and in the second, it both underestimated t_{psim} (error of −291%) and yet overestimated the cumulative infiltration after ponding. For the SCL soil case, characterized by the lowest hydraulic conductivity and infiltrability, the TCA method also underestimated t_{psim} (error of −277%) and overestimated the cumulative infiltration after ponding, as found for the L soil, but the differences are smaller.

[28] The proposed direct method to estimate the ponding time (equation (6)) is illustrated in Figure 4. Three curves are shown in Figure 4 (top): the rainfall intensity versus the cumulative rainfall, $r(R)$; the simulated infiltration capacity curve versus the cumulative infiltration capacity, $f_{cap}(F_{cap})$; and the actual simulated infiltration curve versus the cumulative infiltration, $f_{sim}(F_{sim})$ corresponding to the rainfall event. In Figure 4 (bottom), the inverse function of cumulative rainfall versus time, $t(R)$, is plotted, with the abscissa on the same scales between Figures 4 (top) and 4 (bottom). The cumulative depth at which $f_{cap}(F_{cap})$ and $r(R)$ (the two dashed curves) intersect (Figure 4, top) is translated into the estimate of the ponding time, t_{pest}, through the $t(R)$ curve (Figure 4, bottom). The verification of this estimate is carried out using the simulated $f_{sim}(F_{sim})$ curve (solid line). The simulated ponding time t_{psim}, representing the "exact" solution, can be determined from the intersection between $f_{sim}(F_{sim})$ and $r(R)$ (Figure 4, top) and the $t(R)$ curve (Figure 4, bottom). It can be seen that the accuracy of the suggested

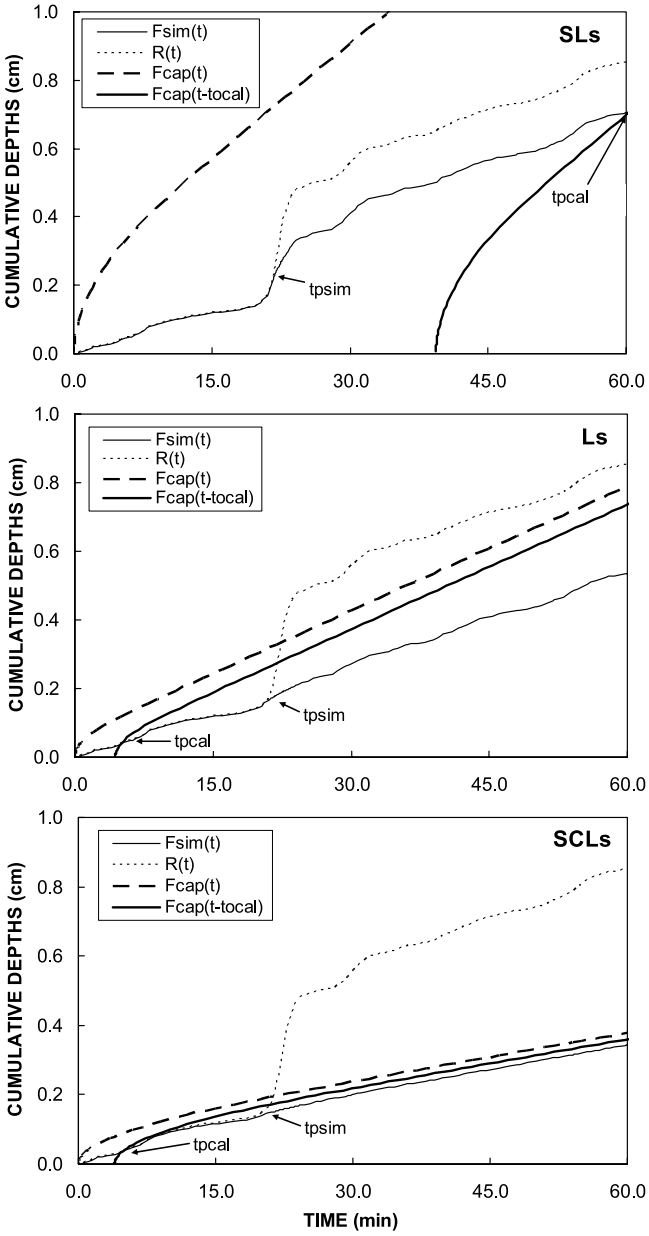

Figure 3. Application of the TCA method to the three soils for the sealed surface condition using equations (13) and (14).

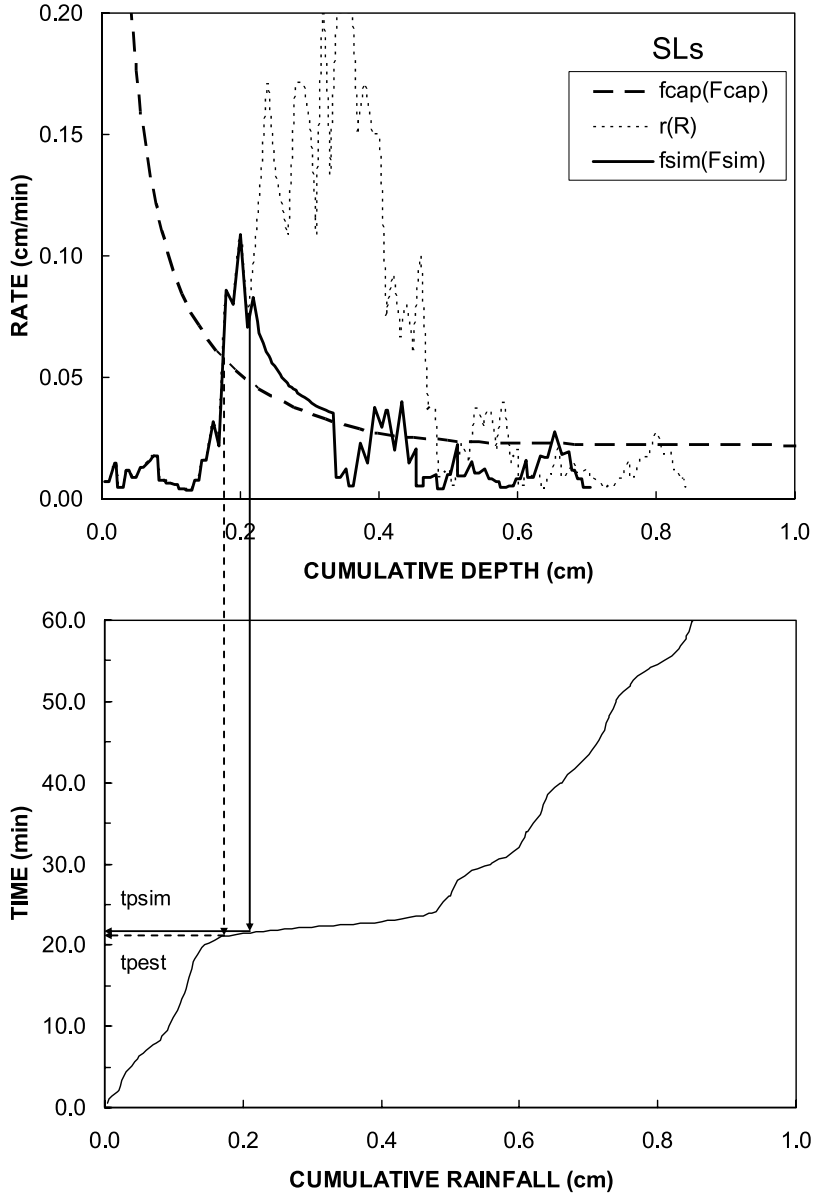

Figure 4. Illustration of the suggested direct method to estimate ponding time (equation (6)) using infiltration capacity and rainfall data (dashed curves in Figure 4, top) and verification of the method using simulated infiltration curve (solid line in Figure 4, top) for the case of the sealed sandy loam soil (SLs).

direct method is good, even when ponding occurred during the steep increase of rainfall intensity.

[29] Graphical presentation of the procedure makes the implementation, which would typically be carried out numerically, easily understood (Figure 4). The graphical construction is as follows: (1) plot, against the same cumulative depth axes, $f_{cap}(F_{cap})$ and $r(R)$; (2) plot the $t(R)$ relationship using the same x axis as in the previous plot and align the origins; (3) use the first plot to determine the value of R at which $r = f_{cap}$; (4) scanning down to the second plot, determine the time corresponding to the previously determined R value, which is t_p.

[30] Following this methodology, the occurrence and timing of ponding is presented for all of the cases considered in this study (Figure 5). It is immediately apparent that ponding will occur for the mulched SCL and for all the sealed surface cases. Estimates of the expected amount of runoff are also readily obtained (equation (12)).

4.2. Effect of Time Interval for Rainfall Intensity Aggregation on Infiltration and Runoff

[31] The suggested approach also offers the possibility to estimate the effect of temporal variability of rainfall on ponding and runoff. This is demonstrated by considering the effect of representing the rainfall event discussed above using temporally averaging over 5, 15, and 60 minute intervals. In Figure 6, the $f_{cap}(F_{cap})$ for the mulched and the sealed SCL soil cases (those that produced runoff using the continuous time record) are plotted along with the $r(R)$ curves. When the soil is mulched, no runoff is predicted using the 60-min and the 15-min time intervals, while some (but still far less than with the complete data set) is predicted based on the 5-min time averaged data. When the soil

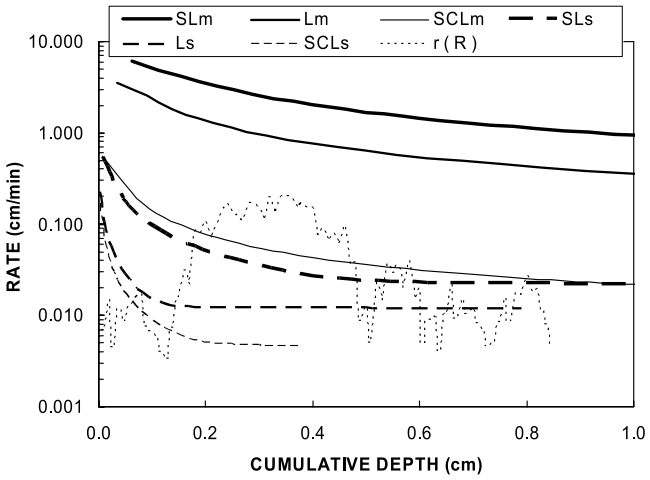

Figure 5. Infiltration capacity curves versus cumulative infiltration, $f_{cap}(F_{cap})$ for the three soils and the two soil surface conditions along with the rainfall rate versus the cumulative rainfall *r(R)*.

surface is sealed, runoff is produced for all the rainfall data sets; however the time averaging interval affects the estimated ponding time and the expected amount of runoff produced.

[32] The effect of the averaging interval is also apparent in the time evolution of the capillary head at the soil surface during rainfall (Figure 7). A monotonic power-like increase of head is seen in the case where the rainfall intensity is constant. When the temporal variability of rainfall intensity is accounted for, the evolving head is no longer either smooth or monotonic, with significant dependence on the time averaging applied, with most dramatic discrepancies during the brief high-intensity periods of the storm. As the time averaging interval decreases, a higher peak value of head is simulated. This can be of importance when infiltration during subsequent rainfall events has to be considered since accounting for temporal variability of rainfall can affect the initial conditions in the soil profile at the consecutive rainfall event. For the sealed condition (Figure 7, bottom) the constant rainfall intensity leads to head at the surface ≤ -20 cm and no runoff, of the more resolved rainfall intensities produce ponding (head=0) and hence runoff, though the time to ponding is different and related to the averaging time interval. The differences at low rainfall intensities are larger for the sealed than for the mulched soil. The impact on subsequent rainfall events may also be expected to be greater in sealed soils.

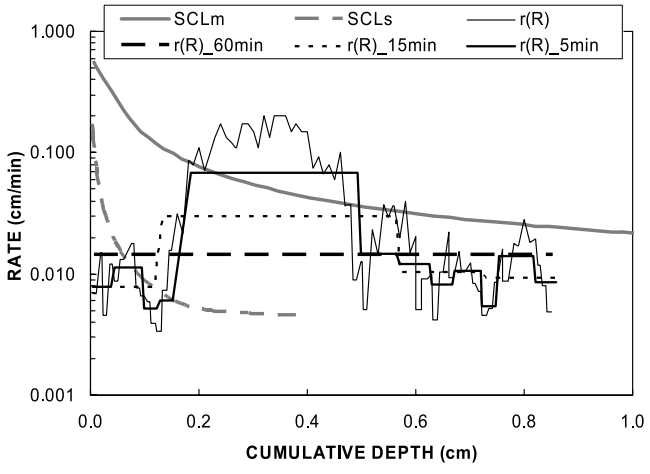

Figure 6. Infiltration capacity curves versus cumulative infiltration, $f_{cap}(F_{cap})$ for the mulched and sealed Atwood soil (SCLm and SCLs) along with the rainfall rate versus the cumulative rainfall curves representing the continuously measured rainfall and aggregated over 5, 15, and 60 min intervals.

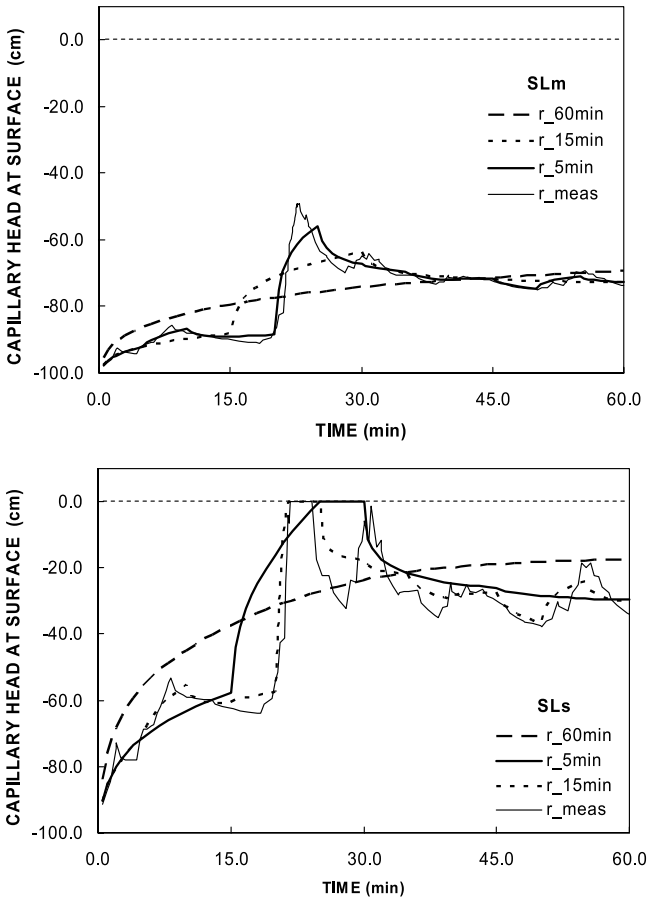

Figure 7. Time evolution of the capillary head at the soil surface during rainfall for the (top) mulched (SLm) and (bottom) sealed (SLs) Sharon sandy loam soil for the continuous and aggregated rainfall.

[33] The simulated cumulative infiltration curves corresponding to the case depicted in Figure 7 (bottom) are shown in Figure 8 along with the cumulative rainfall for the different averaging time intervals. For the constant rainfall intensity, the two lines are linear and coincide exactly, as expected since no runoff was simulated. As the averaging time interval decreases, the departure of the cumulative infiltration from the cumulative rainfall increases and more runoff is "produced" for the same rainfall event.

[34] To summarize, the effects of the time averaging interval on the estimated ponding time and total runoff (Figure 9) may be presented relative to the values obtained

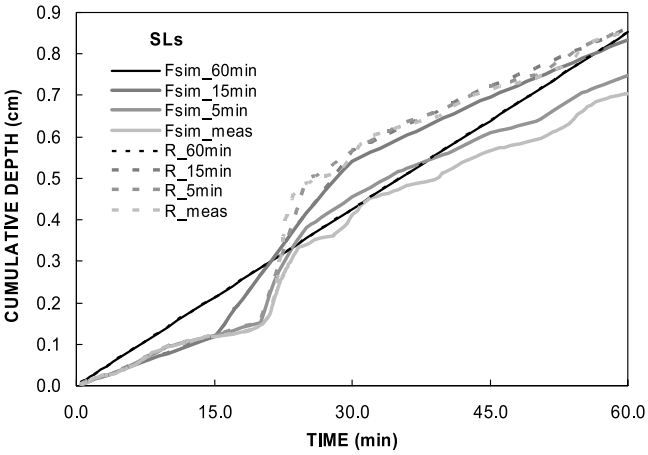

Figure 8. Time evolution of the cumulative rainfall corresponding to the measured and aggregated rainfall with the simulated cumulative infiltration curves versus time, $F_{sim}(t)$, for the SLs case.

using the numerical simulation. Employing an averaging time of 60 min always underestimated ponding time, with an error of around 50% for the loam soil case (Figure 9, top). The averaging time interval of 5-min allows a relatively accurate estimate of t_p, while the effect of the intermediate time averaging interval of 15-min varies with the soil type. For the sealed SL and SCL soils, it causes to a strong overestimation of t_p, the error in the case of the SCL soil being of 100%. For the sealed loam soil, it underestimates it, and the error is around 25%.

[35] The effect on the relative total runoff (Figure 9, bottom) is consistent in greater underestimation with increasing averaging time. The trend, however, is soil type and soil surface dependent. The impact of the time averaging interval is negligible for the sealed Atwood soil but huge for the sealed sandy loam or the mulched Atwood soil. It appears to be convex for the soils with the higher conductivity (infiltrability), and concave for the lower-conductivity soils. In both cases, the errors can be substantial: for the mulched SCL soil, only 46% of the simulated runoff are produced by the 5-min averaged rainfall data, and 75%, for the sealed SL soil, while for the L soil, 78% of the simulated total runoff is produced by the 15-min averaged data, and 87%, when the 5-min averaged data are used.

[36] The scaled $t_{p+}(r_{p+})$ values, using equation (11), that were estimated using the simulated infiltration curves were compared to those resulting from the new method (equation (6)) and to those obtained from the traditional approach (equation (13)) (Figure 10, top). The calculated $t_{p+}(r_{p+})$ curve (equation (13)), which assumes a constant rainfall intensity prior to ponding, underestimates ponding time for all but one case, typically with error on the order of a factor of 10. The mean error was computed according to:

$$ME = \frac{\sum_{1}^{k} \left| t_{p+est} - t_{p+sim} \right| / t_{p+sim}}{k} \qquad (15)$$

where k is the number of points in the sample. The mean error was 87% for the calculated t_{p+} using equation (13) and dropped to 7% for the suggested method (equation (6)). The relationship given by equation (13) is best up to $r_{p+} = 20.0$ where errors are less frequently less than a factor of 10, but above this value the predictions are essentially without predictive significance.

[37] The scaled t_{0+} values estimated by the direct method (equations (6) and (14)) and calculated using equations (13) and (14) are plotted versus the scaled corresponding simulated values (Figure 10, bottom). The comparison between the calculated and simulated t_{0+} values makes clear the dramatically improved performance of the direct method presented here to estimate t_p while accounting for temporal variability of rainfall intensity, in which ME (equation (15)) for the new method is 10%, while the traditional method yields ME of 56% for the cases considered here.

5. Summary and Conclusions

[38] We have proposed an accurate and practical method of using a comparison of the integrated rainfall versus the integrated infiltration capacity to predict the time to ponding

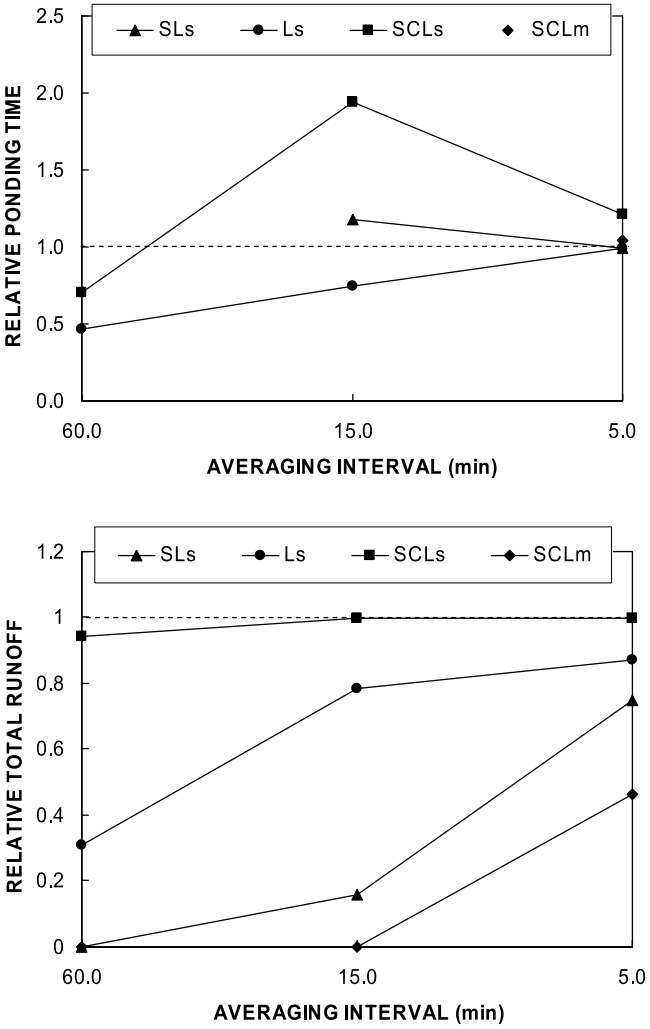

Figure 9. Summary plots of the effects of the time averaging interval on (top) the estimated ponding time and (bottom) total runoff, presented relative to the values obtained using the numerical simulation.

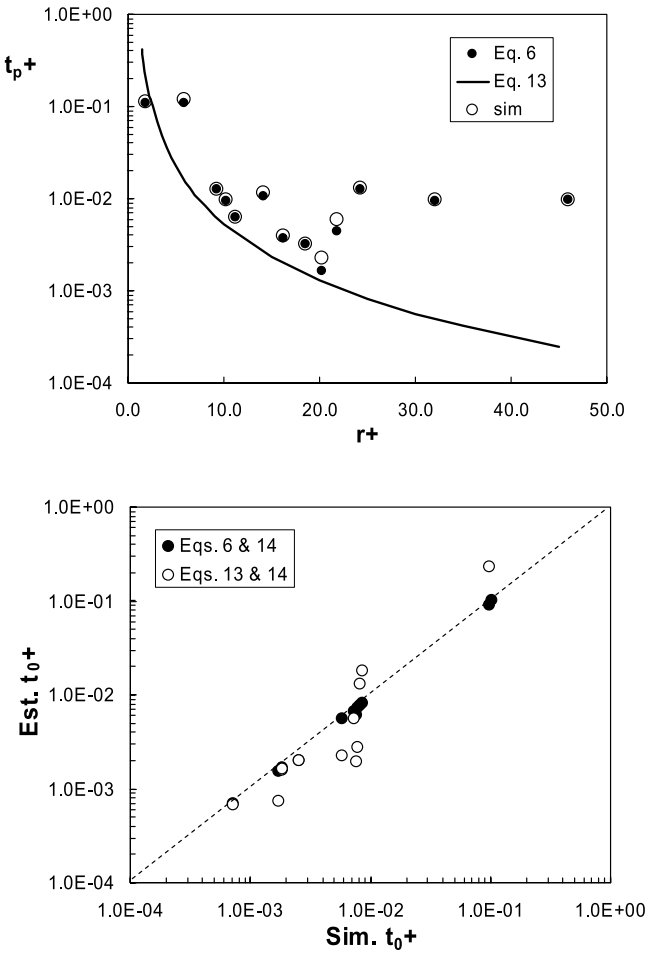

Figure 10. (top) Scaled $t_{p+}(r_{p+})$ values obtained using the simulated infiltration (open circles), those from the new method (solid circles) and the prediction obtained using the traditional approach (solid line). (bottom) Scaled t_{0+} values estimated by the direct method (solid circles) and calculated using equations (13) and (14) (open circles) versus the scaled corresponding simulated values.

and the subsequent excess rainfall. The method builds directly on a wealth of previous related work, but with several significant improvements. The calculations themselves are greatly simplified, since the method is explicit, therefore not requiring iterative estimation of the time to ponding. The approach also allows direct calculation of excess rainfall. Finally, the method requires no particular pattern to rainfall events, while most previous analytical methods were quite restrictive in this aspect. The comparison of the predictions of this simple approach to precise numerical simulations provides striking support for this approach over traditional TCA with respect to the accuracy of the predictions obtained. While the time to ponding using the suggested method had a mean error of 7%, the traditional methods had errors that include complete lack of prediction of ponding, and in many cases, predictions of the time from start of rainfall to ponding that were in error by a factor of 10. It is clear there are conditions in which the two approaches would be indistinguishable in performance (e.g., constant rainfall rate). Though our testing of the comparative performance of the new method to the standard TCA was by no means comprehensive, considering only a very small set of rainfall patterns, it appears that the precision afforded justifies serious reconsideration of use of the techniques that have heretofore been standard. Further exploration of possible errors for specific rainfall-soil conditions is needed to gain reliable assessment of the accuracy of the proposed model, with particular emphasis on the wide range of rainfall patterns observed in the diverse climatic systems where such an approach might be applied.

[39] An area of further research need that is particularly evident is that of the affect of antecedent soil moisture on time to ponding and infiltration. Clearly rainfall often occurs in sequences of closely spaced events, thus resolution of this issue is critical to the advancement of these concepts to many rainfall records. Can one simply integrate the water content over the characteristic capillary length scale of the soil and employ this as effective cumulative infiltration with the method we have proposed? The success of this approach thus far suggests that the issue of antecedent water content may well be amenable to an analytical approach, in which case quite accurate prediction of runoff to rainfall might be tractable as well.

[40] **Acknowledgments.** This study was performed during a joint visit of the authors to the EPFL, Lausanne. The authors thank the School of Architecture, Civil and Environmental Engineering (ENAC) and the directors of the sponsoring laboratories (M. Parlange, D. Or, and A. Barry) for their support and outstanding hospitality.

References

Agnese, C., and V. Bagarello (1997), Describing rate variability of storm events for infiltration prediction, *Trans. ASAE*, *40*, 61–70.

Ahuja, L. R. (1983), Modeling infiltration into crusted soils by the Green-Ampt approach, *Soil Sci. Soc. Am. J.*, *47*, 412–418.

Assouline, S. (2004), Rainfall-induced soil surface sealing: A critical review of observations, conceptual models and solutions, *Vadose Zone J.*, *3*, 570–591.

Assouline, S., and Y. Mualem (1997), Modeling the dynamics of seal formation and its effect on infiltration as related to soil and rainfall characteristics, *Water Resour. Res.*, *33*, 1527–1536.

Assouline, S., and Y. Mualem (2001), Soil seal formation and its effect on infiltration: Uniform versus nonuniform seal approximation, *Water Resour. Res.*, *37*, 297–305.

Assouline, S., and Y. Mualem (2002), Infiltration during soil sealing: The effect of areal heterogeneity of soil hydraulic properties, *Water Resour. Res.*, *38*(12), 1286, doi:10.1029/2001WR001168.

Baumhardt, R. L., M. J. M. Romkens, F. D. Whisler, and J. Y. Parlange (1990), Modeling infiltration into a sealing soil, *Water Resour. Res.*, *26*, 2497–2505.

Beven, K. (1984), Infiltration into a class of vertically non-uniform soils, *Hydrol. Sci. J.*, *29*, 425–434.

Broadbridge, P., and I. White (1987), Time to ponding: Comparison of analytic, quasi-analytic, and approximate predictions, *Water Resour. Res.*, *23*, 2302–2310.

Brooks, R. H., and A. T. Corey (1964), Hydraulic properties of porous media, *Hydrol. Pap. 3*, 27 pp., Colo. State Univ., Fort Collins.

Brutsaert, W. (2005), *Hydrology: An Introduction*, Cambridge Univ. Press, New York.

Childs, E. C., and M. Bybordi (1969), The vertical movement of water in stratified porous material: 1. Infiltration, *Water Resour. Res.*, *5*, 446–459.

Chow, V. T., D. R. Maidment, and L. W. Mays (1988), *Applied Hydrology*, McGraw-Hill, New York.

Chu, X., and M. A. Marino (2005), Determination of ponding condition and infiltration into layered soils under unsteady conditions, *J. Hydrol.*, *313*, 195–207.

Clothier, B. E. (2001), Infiltration, in *Soil and Environmental Analysis: Physical Methods*, 2nd ed., edited by K. A. Smith and C. E. Mullins, pp. 239–280, CRC Press, Boca Raton, Fla.

Frauenfeld, B., and C. Truman (2004), Variable rainfall intensity effects on runoff and interrill erosion from two coastal plain ultisols in Georgia, *Soil Sci.*, *169*, 143–154.

Govindaraju, R. S., C. Corradini, and R. Morbidelli (2006), A semi-analytical model of expected areal-average infiltration under spatial heterogeneity of rainfall and soil saturated hydraulic conductivity, *J. Hydrol.*, *316*, 184–194.

Green, W. A., and G. A. Ampt (1911), Studies on soils physics: 1. The flow of air and water trough soils, *J. Agric. Sci.*, *4*, 1–24.

Hillel, D. (2004), *Introduction to Environmental Soil Physics*, Elsevier, New York.

Hillel, D., and W. R. Gardner (1970), Transient infiltration into crust topped profiles, *Soil Sci.*, *109*, 69–76.

Holtan, H. N. (1945), Time condensation in hydrograph analysis, *Eos Trans. AGU*, *26*, 407–413.

Hopmans, J., S. Assouline, and J. Y. Parlange (2006), Infiltration, in *The Handbook of Groundwater Hydrology*, 2nd ed., edited by J. W. Delleur, CRC Press, Boca Raton, Fla.

Horton, R. E. (1940), An approach towards a physical interpretation of infiltration capacity, *Soil Sci. Soc. Am. Proc.*, *5*, 399–417.

Kim, C. P., J. N. M. Stricker, and P. J. J. F. Torfs (1996), An analytical framework for the water budget of the unsaturated zone, *Water Resour. Res.*, *32*, 3475–3484.

Kostiakov, A. N. (1932), On the dynamics of the coefficient of water percolation in soils and on the necessity of studying it from a dynamic point of view for purposes of amelioration, *Trans. Comm. Int. Soc. Soil Sci., Part A, 6th*, 17–21.

Kutilek, M., and D. R. Nielsen (1994), *Soil Hydrology*, 370 pp., Catena, Reiskirchen, Germany.

Mualem, Y. (1976), A new model of predicting the hydraulic conductivity of unsaturated porous media, *Water Resour. Res.*, *12*, 513–522.

Mualem, Y., and S. Assouline (1996), Soil sealing, infiltration and runoff, in *Runoff, Infiltration and Subsurface Flow of Water in Arid and Semi-arid Regions*, edited by A. S. Issar, and S. D. Resnick, Elsevier, New York.

Parlange, J.-Y., and R. E. Smith (1976), Ponding time for variable rainfall rates, *Can. J. Soil Sci.*, *56*, 121–123.

Parlange, J.-Y., W. L. Hogarth, and M. B. Parlange (1984), Optimal analysis of surface crusts, *Soil Sci. Soc. Am. J.*, *48*, 494–497.

Parlange, J.-Y., W. L. Hogarth, D. A. Barry, M. B. Parlange, R. Haverkamp, P. J. Ross, T. S. Steenhuis, D. A. DiCarlo, and G. Katul (1999), Analytical approximation to the solution of Richards' equation with application to infiltration, ponding, and time compression approximation, *Adv. Water. Resour.*, *23*, 189–194.

Philip, J. R. (1957a), The theory of infiltration: 1. The infiltration equation and its solution, *Soil Sci.*, *83*, 345–357.

Philip, J. R. (1957b), The theory of infiltration: 4. Sorptivity and algebraic infiltration equations, *Soil Sci.*, *84*, 257–264.

Reeves, M., and E. E. Miller (1975), Estimating infiltration for erratic rainfall, *Water Resour. Res.*, *11*, 102–110.

Russo, D., and E. Bresler (1982), A univariate versus a multivariate parameter distribution in a stochastic-conceptual analysis of unsaturated flow, *Water Resour. Res.*, *18*, 483–489.

Saghafian, B., P. Y. Julien, and F. L. Ogden (1995), Similarity in catchment response: 1. Stationary rainstorms, *Water Resour. Res.*, *31*, 1533–1541.

Selker, J. S., J. Duan, and J. Y. Parlange (1999), Green and Ampt infiltration into soils of variable pore size with depth, *Water Resour. Res.*, *35*, 1685–1688.

Sherman, L. K. (1943), Comparison of F-curves derived by the method of Sharp and Holtan and of Sherman and Mayer, *Eos Trans. AGU*, *24*, 465–467.

Simunek, J., M. T. van Genuchten, and M. Sejna (2005), The HYDRUS-1D software package for simulating the movement of water, heat, and multiple solutes in variably saturated media, version 3.0, *HYDRUS Software Ser. 1*, 270 pp., Dep. of Environ. Sci., Univ. of Calif., Riverside.

Sivapalan, M., and P. C. D. Milly (1989), On the relationship between the time condensation approximation and the flux-concentration relation, *J. Hydrol.*, *105*, 357–367.

Sivapalan, M., and E. F. Wood (1986), Spatial heterogeneity and scale in the infiltration response of catchments, in *Scale Problems in Hydrology, Water Sci. Technol. Libr.*, vol. 6, edited by V. K. Gupta, I. Rodriguez-Iturbe, and E. F. Wood, pp. 81–106, Springer, New York.

Smith, R. E. (1972), The infiltration envelope: Results from a theoretical infiltrometer, *J. Hydrol.*, *17*, 1–21.

Smith, R. E. (1990), Analysis of infiltration through a two-layer soil profile, *Soil Sci. Soc. Am. J.*, *54*, 1219–1227.

Smith, R. E., and D. L. Chery (1973), Rainfall excess model from soil water flow theory, *J. Hydrol. Div. Am. Soc. Civ. Eng.*, *99*, 1337–1351.

Smith, R. E., and J.-Y. Parlange (1978), A parametric-efficient hydrologic infiltration model, *Water Resour. Res.*, *14*, 533–536.

Smith, R. E., K. R. J. Smettem, P. Broadbridge, and D. A. Woolhiser (2002), *Infiltration Theory for Hydrologic Applications,*, vol. 15, AGU, Washington, D. C.

Strickland, T. C., C. C. Truman, and B. Frauenfeld (2005), Variable rainfall intensity effects on carbon characteristics in eroded sediments from two coastal plain ultisols in Georgia, *J. Soil Water Conserv.*, *60*, 142–148.

van Genuchten, M. T. (1980), A closed-form equation for predicting the hydraulic conductivity of unsaturated soils, *Soil Sci. Soc. Am. J.*, *44*, 892–898.

Wainwright, J., and A. J. Parsons (2002), The effect of temporal variations in rainfall on scale dependency in runoff coefficients, *Water Resour. Res.*, *38*(12), 1271, doi:10.1029/2000WR000188.

Warrick, A. W. (2002), *Soil Physics Companion*, CRC Press, Boca Raton, Fla.

S. Assouline, Institute of Soil, Water and Environmental Sciences, ARO, Volcani Center, P.O. Box 6, Bet Dagan 50250, Israel. (vwshmuel@agri.gov.il)

J.-Y. Parlange, Department of Biological and Environmental Engineering, Riley-Robb Hall, Cornell University, Ithaca, NY 14853, USA. (jp58@cornell.edu)

J. S. Selker Department of Biological and Ecological Engineering, Oregon State University, Corvallis, OR 97331, USA. (selkerj@engr.orst.edu)